A Cable-Driven Parallel Robot With an Embedded Tilt-Roll Wrist

Saman Lessanibahri, Philippe Cardou, Stéphane Caro

**the ASME 2019 International Design Engineering Technical Conferences &
Computers and Information in Engineering Conference
IDETC/CIE 2019
August 18-212019 Anaheim, CaliforniaUSA**

IDETC2019-98146

A CABLE-DRIVEN PARALLEL ROBOT WITH AN EMBEDDED TILT-ROLL WRIST

Saman Lessanibahri[1,2], Philippe Cardou[3], Stéphane Caro[2,4]*
[1] École Centrale de Nantes, Nantes, 44321 France
[2] Laboratoire des Sciences du Numérique de Nantes (LS2N), UMR CNRS 6004, Nantes, 44300, France
[3] Laboratoire de robotique, Département de génie mécanique, Université Laval, Québec, QC, Canada
[4] Centre National de la Recherche Scientifique (CNRS), Nantes, 44321, France
Emails: Saman.Lessanibahri@ls2n.fr
pcardou@gmc.ulaval.ca, Stephane.Caro@ls2n.fr

ABSTRACT

This paper addresses the optimum design, configuration and workspace analysis of a Cable-Driven Parallel Robot with an embedded tilt-roll wrist. The manipulator is a hybrid robot consisting in an under-constrained moving-platform accommodating a tilt-roll wrist. The embedded wrist provides large amplitudes of tilt and roll rotations and a large translational workspace obtained by the moving-platform. This manipulator is suitable for tasks requiring large rotation and translation workspaces like tomography scanning, camera-orienting devices and visual surveillance. The moving-platform is an eight-degree-of-freedom articulated mechanism with large translational and rotational workspaces and it is suspended from a fixed frame by six cables. The manipulator employs two bi-actuated cables, i.e., cable loops to transmit the power from motors fixed on the ground to the tilt-roll wrist. Therefore, the manipulator achieves better dynamic performances due to a lower inertia of its moving-platform.

1 Introduction

Cable-Driven Parallel Robots (CDPRs) consist of a base frame and a moving-platform connected to each other through cables. Cables are actuated by winches connected to motors that can vary cable tensions and lengths. When compared to classical parallel robots, CDPRs have advantages in terms of large translation workspace [1, 2], heavy payload capacity [3], reconfigurability [4] and capability of performing high-speed tasks [5].

Despite their large translation workspaces, CDPRs are mainly unable to provide large amplitudes of rotation of their moving-platforms due to collision between their moving parts. In general, the workspaces of parallel robots can be extended by combining other parallel or serial mechanism to them and constructing hybrid mechanisms. To the best of the authors' knowledge, there is but a limited number of papers addressing the question of extending the rotation workspaces of CDPRs. In [6], a parallel spherical wrist was introduced into the design of a CDPR to obtain large rotation and translation workspaces. The authors showed that the workspace of CDPRs can be enlarged by combining the advantages of the parallel spherical wrist in terms of rotation amplitudes with those of CDPRs in terms of large translation workspace.

Cable-loops or bi-actuated cable circuits are employed for different reasons in the design of several CDPRs, such as increasing the size of wrench-feasible workspace [7–9]. The other application of cable-loops is the actuation of embedded end-effectors on the moving-platforms (hybrid mechanisms) through cable-loops and drums, so that no motor is required to be mounted on the moving-platform. In [10, 11], two concepts of hybrid CDPRs were detailed. In [10], a hoist was combined with a CDPR, with granted large rotation amplitudes of the hoist for adjusting height of a payload. In the latter paper, the concept of a CDPR, with large translational workspace and large tilt and roll

*Address all correspondence to this author.

rotations of its end-effector was introduced. Hybrid mechanisms generally undergo reduced kinematic and dynamic performance due to their design complexity and high inertia of the moving-platform. However, by employing cable-loops into the design of hybrid CDPRs, the latter adverse effects are minimum.

The cable-loop has two distinct purposes for the CDPR with embedded tilt-roll wrist. The former is devoted to the positioning of the moving-platform and the latter is reserved for the actuation of the tilt-roll wrist. The cable-loops transmit power directly from motors attached on the ground to the articulated moving-platform. This contributes to the lower inertia properties of the moving-platform and better dynamic performance of the manipulator.

Figure 1 shows the overall schematic of the manipulator and Fig. 2 represents the schematic of the moving-platform with the embedded tilt-roll wrist. Figure 3 illustrates the section-view of the moving-platform with their main components as $\mathscr{P}_i$, $i = 1, ..., 5$. The proposed manipulator consists of the base frame, namely, $\mathscr{P}_0$, an under-constrained moving-platform, $\mathscr{P}_1$, which is suspended by six cables. Two bi-actuated cables and four uni-actuated cables are illustrated in Fig. 1. Each cable loop forms a circuit by connecting two actuators while passing through two anchor points on the moving-platform and coiling about a gear on the tilt-roll wrist. Two motions can be induced by the cable-loop depending on the relative rotation of its two actuators. The first one is the displacement of the moving-platform for identical inputs to the two motors. The second motion is the rotation of the gears $\mathscr{P}_3$ and $\mathscr{P}_4$ about their respective axes (z_3 and z_4) as shown in Fig. 2, when the two actuators rotate in opposite directions.

The study of optimum design and configuration of the CDPR with an embedded tilt-roll wrist providing large translational and rotational workspaces is divided into the following sections. Section 2 presents the kinetostatic model of the manipulator. Section 3 studies the static workspace analysis and its calculation. The optimum design and cable configuration of the moving-platform are discussed in Sec. 4. Section 5 presents the result and the workspace of the optimum design of the moving-platform. Design and prototyping of the proposed moving-platform is presented in Sec. 6. Section 7 and the last section concludes the paper.

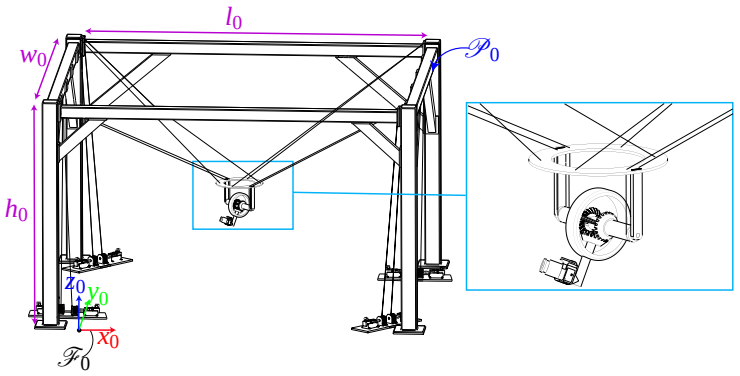

FIGURE 1: Schematic of the manipulator

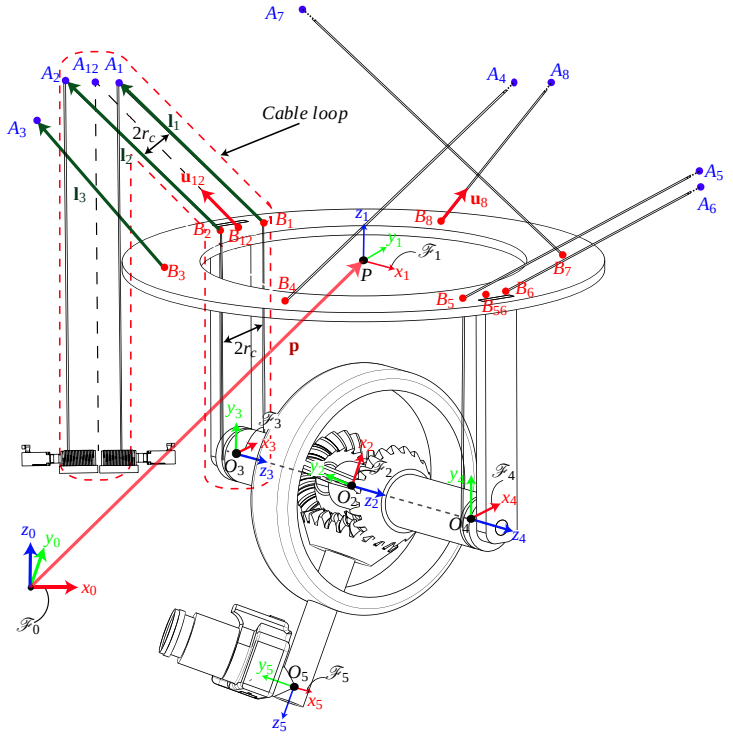

FIGURE 2: Schematic of the moving-platform with an embedded tilt-roll wrist

2 Kinetostatic Model of the Manipulator

In this section, we present the kinetostatic model of the overall manipulator. In order to define the manipulator wrench matrix, we first introduce the loop-closure equations of the CDPR, which are given by:

$$ {}^0\mathbf{l}_i = {}^0\mathbf{a}_i - {}^0\mathbf{p} - {}^0\mathbf{R}_1\,{}^1\mathbf{b}_i, \quad i = 1, 2, ..., 8 \tag{1} $$

where ${}^0\mathbf{l}_i$ is the ith cable vector, i.e., the Cartesian coordinate vector pointing from point B_i to point A_i. Points A_i and B_i stand for the ith cable exit point and anchor point, respectively. The former point is the location of the ith pulley fixed to the ceiling and the latter is the connection point between the cable and the moving-platform. ${}^0\mathbf{a}_i = [a_{ix}, a_{iy}, a_{iz}]^T$, ${}^1\mathbf{b}_i = [b_{ix}, b_{iy}, b_{iz}]^T$ and ${}^0\mathbf{p} = [p_x, p_y, p_z]^T$ are the Cartesian coordinate vectors of points A_i, B_i and P, respectively. ${}^0\mathbf{R}_1$ is the rotation matrix from frame $\mathscr{F}_0$ to frame $\mathscr{F}_1$. And $\mathbf{t}_i$, $i = 1, 2, ..., 8$, stands for the ith cable

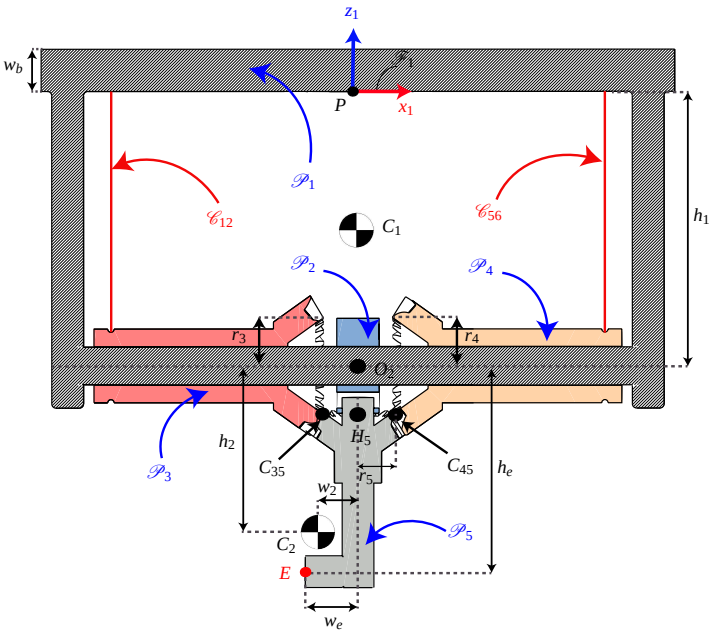

FIGURE 3: Section-view of the moving-platform and the tilt-roll wrist

tension vector. $\mathbf{t}_i = t_i {}^0\mathbf{u}_i$ and its magnitude is expressed as $t_i = \|\mathbf{t}_i\|_2$, $i = 1, ..., 8$. ${}^0\mathbf{u}_i$ denotes the ith cable unit vector namely,

$$ {}^0\mathbf{u}_i = \frac{{}^0\mathbf{l}_i}{l_i}, \quad i = 1,\ 2,\ ...,\ 8 \tag{2} $$

l_i being the ith cable length.

In the modeling, a single virtual cable substitutes each cable-loop. The latter virtual cables replace each cable-loop with A_i and B_i, $i = 12,\ 56$, as their exit point and anchor points, respectively. As long as the moving-platform is far from points A_1 and A_2, then A_1B_1 and A_2B_2 can be assumed parallel and the virtual cable model replaces the first cable-loop. This analogy also holds for the second cable-loop. Therefore, the effect of the first cable-loop onto the moving-platform is the force passing through the midpoint B_{12} between B_1 and B_2 along the unit vector $\mathbf{u}_{12}$ of segment $A_{12}B_{12}$. $\mathbf{t}_{12} = \mathbf{t}_1 + \mathbf{t}_2$ is the tension resultant in the first cable loop. The Cartesian coordinates of the exit and anchor points in both the cable-loops are:

$$ \mathbf{a}_{12} = (\mathbf{a}_1 + \mathbf{a}_2)/2 \tag{3} $$
$$ \mathbf{a}_{56} = (\mathbf{a}_5 + \mathbf{a}_6)/2 \tag{4} $$

and,

$$ \mathbf{b}_{12} = (\mathbf{b}_1 + \mathbf{b}_2)/2 \tag{5} $$
$$ \mathbf{b}_{56} = (\mathbf{b}_5 + \mathbf{b}_6)/2 \tag{6} $$

The equilibrium of the external forces applied on the moving-platform is formulated as follows:

$$ \sum t_i {}^0\mathbf{u}_i + m\mathbf{g} = 0, \quad i = 1, ..., 8, \tag{7} $$

where $m\mathbf{g}$ is the weight of the moving-platform. m denotes total mass of the moving-platform and the spherical wrist. The equilibrium of moments applied onto the moving-platform about point P expressed in frame $\mathscr{F}_0$ takes the form:

$$ \sum t_i \left({}^0\mathbf{R}_1 {}^1\mathbf{b}_i \times {}^0\mathbf{u}_i \right) + m({}^0\mathbf{c} - {}^0\mathbf{p}) \times {}^0\mathbf{g} = 0, \quad i = 1, ..., 8 \tag{8} $$

with $\mathbf{c}$ being the Cartesian coordinates vector of the Center of Mass (CoM) of the moving-platform:

$$ \mathbf{c} = \frac{m_1\mathbf{c}_1 + m_2\mathbf{c}_2}{m_1 + m_2} \tag{9} $$

$\mathbf{c}_1$ stands for the CoM of components $\mathscr{P}_1$ to $\mathscr{P}_4$ of mass of m_1 and $\mathbf{c}_2$ denotes the CoM of $\mathscr{P}_5$ of mass of m_2. Therefore, overall mass of the moving-platform is expressed as follows:

$$ m = m_1 + m_2 \tag{10} $$

The input tilt-roll wrist torques τ_3 and τ_4 are function of the cable tension difference in cable-loops $\mathscr{C}_{12}$ and $\mathscr{C}_{56}$, respectively:

$$ \tau_3 = r_c (t_1 - t_2) \tag{11} $$
$$ \tau_4 = r_c (t_6 - t_5) \tag{12} $$

r_c being the radius of the groove made in $\mathscr{P}_3$ and $\mathscr{P}_4$ to house the two cable-loops. From Eqs. (7) to (12) the static equilibrium model of the manipulator is expressed in a matrix form as:

$$ \mathbf{W}\mathbf{t} + \mathbf{w}_g = \mathbf{0}_8 \tag{13} $$

where $\mathbf{0}_8$ is an eight-dimensional zero vector and the wrench matrix $\mathbf{W}$ takes the following form:

$$ \mathbf{W} = \begin{bmatrix} {}^0\mathbf{u}_1 & {}^0\mathbf{u}_2 & {}^0\mathbf{u}_3 & {}^0\mathbf{u}_4 & {}^0\mathbf{u}_5 & {}^0\mathbf{u}_6 & {}^0\mathbf{u}_7 & {}^0\mathbf{u}_8 \\ {}^0\mathbf{d}_1 & {}^0\mathbf{d}_2 & {}^0\mathbf{d}_3 & {}^0\mathbf{d}_4 & {}^0\mathbf{d}_5 & {}^0\mathbf{d}_6 & {}^0\mathbf{d}_7 & {}^0\mathbf{d}_8 \\ r_c & -r_c & 0 & 0 & -r_c & r_c & 0 & 0 \\ \mu r_c & -\mu r_c & 0 & 0 & \mu r_c & -\mu r_c & 0 & 0 \end{bmatrix} \tag{14} $$

with $\mu = \frac{r_5}{r_3} = \frac{r_5}{r_4}$ being the gear train ratio and the pitch radius of ith gear is denoted as r_i and $i = 3,\ 4,\ 5$. And,

$$ {}^0\mathbf{d}_i = {}^0\mathbf{R}_1\,{}^1\mathbf{b}_i \times {}^0\mathbf{u}_i, \quad i = 1, ..., 8 \tag{15} $$

The last two rows of $\mathbf{W}$ correspond to the static model of the tilt-roll wrist presented in kinetostatic model of the tilt-roll wrist of [11]. $\mathbf{t}$ is the vector containing the tensions exerted by the eight actuators to the cables.

$$ \mathbf{t} = [t_1\ \ t_2\ \ t_3\ \ t_4\ \ t_5\ \ t_6\ \ t_7\ \ t_8]^T \tag{16} $$

$\mathbf{w}_g$ is the eight-dimensional gravity wrench vector applied on the moving-platform and the tilt-roll wrist, namely,

$$ \mathbf{w}_g = [m\,{}^0\mathbf{g}^T \quad m({}^0\mathbf{R}_1\,{}^1\mathbf{c} \times {}^0\mathbf{g})^T\ \ \mathbf{m}_{\alpha,\beta}^T]^T \tag{17} $$

where,${}^0\mathbf{g} = [0,\ 0,\ -g]^T$ with $g = 9.81\ m.s^{-2}$.

$$ m_1 = m_b + 2m_c + m_s + m_{\mathscr{P}_2} + m_{\mathscr{P}_3} + m_{\mathscr{P}_4} \tag{18} $$

m_b, m_c and m_s being the masses of the moving-platform components such as, base, columns and shaft, respectively. Coordinate vector of C_1 expressed in $\mathscr{F}_1$ is denoted as ${}^1\mathbf{c}_1$ as follows:

$$ {}^1\mathbf{c}_1 = [0,\ 0,\ c_{1z}]^T \tag{19} $$

with,

$$ c_{1z} = \frac{-h_1(m_c + m_s + m_{\mathscr{P}_2} + m_{\mathscr{P}_3} + m_{\mathscr{P}_4})}{m_1} \tag{20} $$

and variable coordinate vector of CoM, namely, C_2 is a function of α and β as follows:

$$ {}^1\mathbf{c}_2 = \begin{bmatrix} -w_2 \sin\beta \\ -h_2 \cos\alpha - w_2 \sin\alpha \cos\beta \\ -h_2 \sin\alpha + w_2 \cos\alpha \cos\beta - h_1 \end{bmatrix} \tag{21} $$

The tilt angle of the end-effector is denoted as $\alpha = \angle(y_1,\ x_2)$ and the roll angle is defined as $\beta = \angle(z_2,\ x_5)$. $\mathbf{m}_{\alpha,\beta}$ is the gravitational moments applied by environment onto the tilt-roll wrist about z_2 and z_5, respectively.

$$ \mathbf{m}_{\alpha,\beta} = [m_\alpha,\ m_\beta]^T \tag{22} $$

with $m_\alpha = m_{g_z}$ and $m_\beta = -m_{g_x}$. The moment due to the weight of $\mathscr{P}_5$ exerted on the tilt-roll wrist expressed in $\mathscr{F}_2$ is denoted as ${}^2\mathbf{m}_g = \left[m_{g_x},\ m_{g_y},\ m_{g_z}\right]^T$.
with,

$$ {}^2\mathbf{m}_g = m_2\left({}^2\mathbf{c}_2 \times {}^2\mathbf{R}_0\,{}^0\mathbf{g}\right) = m_2 g \begin{bmatrix} -w_2 \sin\beta \cos\alpha \\ w_2 \sin\beta \sin\alpha \\ h_2 \cos\alpha + w_2 \cos\beta \sin\alpha \end{bmatrix} \tag{23} $$

3 Workspace Analysis

In this section, we introduce the static workspace of the CDPR with an embedded tilt-roll wrist. In general, the static workspace of the eight-DoF CDPR with embedded tilt-roll wrist consist of set of positions and orientations of the moving-platform and the orientations of the end-effector, namely, ${}^0\mathbf{p}$ and ${}^0\mathbf{R}_1$ and $\mathbf{q}_{TR} = [\alpha,\ \beta]^T$ which satisfies the static equilibrium of the manipulator. The set $\mathscr{T}$ forms the feasible cable tensions as a box in eight-dimensional space:

$$ \mathscr{T} = \{\mathbf{t} \in \mathbb{R}^8 :\ \mathbf{t}_{min} \leq \mathbf{t} \leq \mathbf{t}_{max}\}. \tag{24} $$

where, $\mathbf{t}_{min}$ and $\mathbf{t}_{max}$ are the lower and upper bounds of admissible cable tensions. Static Workspace (SW), namely, $\mathscr{S}$ is set of the moving-platform poses and tilt-roll wrist configurations satisfying the static equilibrium of the manipulator with admissible cable tensions.

$$ \mathscr{S} = \{({}^0\mathbf{p}, {}^0\mathbf{R}_1, \mathbf{q}_{TR}) \in \mathbb{R}^3 \times SO(3) \times \mathbb{R}^2 : \exists \mathbf{t} \in \mathscr{T},\ \mathbf{W}\mathbf{t} + \mathbf{w}_g = \mathbf{0}_8\} \tag{25} $$

where $SO(3)$ is the group of proper rotation matrices. As illustration of such workspace is not straightforward in Cartesian space, we define the SW of the manipulator for two different cases. Therefore, from Eq. (25) we derive two subsets $\mathscr{S}_1$ and $\mathscr{S}_2$ based on the constrained orientations of the moving-platform and the tilt-roll wrist. The former subset, namely, $\mathscr{S}_1$ is a set for a given orientation of the moving-platform and the wrist, i.e., the translational SW of the manipulator with constant orientation of ${}^0\mathbf{R}_1$ and $\mathbf{q}_{TR}$.

$$ \mathscr{S}_1 = \{{}^0\mathbf{p} \in \mathbb{R}^3 \,|\, {}^0\mathbf{R}_1 = \mathbf{I}_3,\ \alpha = \beta = \pi/2 : \exists \mathbf{t} \in \mathscr{T},\ \mathbf{W}\mathbf{t} + \mathbf{w}_g = \mathbf{0}_8\} \tag{26} $$

The minimum moment due to weight of $\mathscr{P}_5$ exerted on the tilt-roll wrist corresponds to $\alpha = \beta = \pi/2$. Therefore, for largest possible workspace of $\mathscr{S}_1$ we consider those angles for tilt and roll of the wrist. $\mathscr{S}_2$ amounts to the SW of the manipulator for a constant orientation of the moving-platform while the tilt and

roll is free to rotate.

$$\mathscr{S}_2 = \{{}^0\mathbf{p} \in \mathbb{R}^3 \,|\, {}^0\mathbf{R}_1 = \mathbf{I}_3 : -\pi \leq \alpha \,\&\, \beta \leq \pi : \exists \mathbf{t} \in \mathscr{T},\ \mathbf{W}\mathbf{t} + \mathbf{w}_g = \mathbf{0}_8\} \tag{27}$$

In order to trace the SW, an index, namely, capacity margin is employed for identification of static equilibrium of the moving-platform for a given pose. In [12] and [13] the capacity margin index was introduced and implemented for tracing wrench feasible workspace and static equilibrium of the CDPRs. In the latter papers the algorithm of calculation of capacity margin is detailed.

Hereafter, the capacity margin index can be checked to indicates whether any given pose of the moving-platform belongs to SW or not. By discretization of the Cartesian space and checking them through the index, we are able to trace the static workspace. The discretization of Cartesian space is detailed in the following.

$$x_i = x_0 + i\,\delta \quad (i = 0,\ ...,\ n_x) \tag{28}$$
$$y_j = y_0 + j\,\delta \quad (j = 0,\ ...,\ n_y) \tag{29}$$
$$z_k = z_0 + k\,\delta \quad (k = 0,\ ...,\ n_z) \tag{30}$$

with δ being the resolution of the discretization and $\mathbf{o}_0 = [x_0,\ y_0,\ z_0]^T$ denotes the origin of frame $\mathscr{F}_0$. And the number of discretized points along x, y and z are detailed in the following, respectively.

$$n_x = \left\lfloor \frac{l_0 - x_0}{\delta} \right\rfloor \tag{31}$$
$$n_y = \left\lfloor \frac{w_0 - y_0}{\delta} \right\rfloor \tag{32}$$
$$n_z = \left\lfloor \frac{h_0 - z_0}{\delta} \right\rfloor \tag{33}$$

where, l_0, w_0 and h_0 are length, width and height of the manipulator frame ($\mathscr{P}_0$), respectively. Number of points found to be inside the SW, $\mathscr{S}_1$ and $\mathscr{S}_2$ are denoted as $N_{\mathscr{S}_1}$ and $N_{\mathscr{S}_2}$ as follows:

$$N_{\mathscr{S}_1} = \left|\left\{\mathbf{p}\left(x_i,\ y_j,\ z_k\right) \in \mathscr{S}_1\right\}\right| \tag{34}$$
$$N_{\mathscr{S}_2} = \left|\left\{\mathbf{p}\left(x_i,\ y_j,\ z_k\right) \in \mathscr{S}_2\right\}\right| \tag{35}$$

with x_i, y_i and z_i being defined in Eqs. (28-30). Ratio of SWs, namely $\mathscr{R}_{\mathscr{S}_i}$, $i = 1, 2$, is introduced to quantify the proportion of $\mathscr{S}_1$ and $\mathscr{S}_2$ to the task space, respectively.

$$\mathscr{R}_{\mathscr{S}_1} = \frac{N_{\mathscr{S}_1}}{(n_x+1)(n_y+1)(n_z+1)} \tag{36}$$
$$\mathscr{R}_{\mathscr{S}_2} = \frac{N_{\mathscr{S}_2}}{(n_x+1)(n_y+1)(n_z+1)} \tag{37}$$

4 Optimum Design of the Cable-Driven Parallel Robot using a Tilt-Roll Wrist

This section deals with optimization of the CDPR with the embedded tilt-roll wrist. The investigation of the optimum manipulator focuses on two goals. The first one deals with the determination of the optimum cable arrangement. The second goal is devoted to the search of the optimum design variables of the moving-platform. The following formulates the problem of the optimum design of the CDPR with an embedded tilt-roll wrist. It expresses the main parts of the optimization problem in terms of objective function, decision variables and constraints.

$$\begin{aligned} \text{maximize} \quad & f(\mathbf{x}) = \mathscr{R}_{\mathscr{S}_2} \\ \text{over} \quad & \mathbf{x} = [r_b,\ h_1,\ w_b,\ \theta_c,\ \theta_u,\ \eta]^T \\ \text{subject to:} \quad & \\ & g_1 :\ {}^1e_z(\alpha_h,\ \beta_h) < 0 \\ & g_2 :\ m < 5\ kg \\ & \mathbf{x}_{lb} \leq \mathbf{x} \leq \mathbf{x}_{ub} \end{aligned} \tag{38}$$

The design variables expressed in Table 1 are searched for the given design parameters mentioned in Table 2. This section deals with optimum design of the moving-platform to maximize the volume of the static workspace, $\mathscr{R}_{\mathscr{S}_2}$. The decision variables describe the overall dimensions of the moving-platform while those of the tilt-roll wrist are considered as design parameters. The positions of the anchor points on $\mathscr{P}_1$ are also considered as decision variables in order to determine the optimum cable configuration of the CDPR.

Objective Function

Cable-loops and tilt-roll wrist have significant effects on the size and shape of the SW. The expected task of the manipulator is for its moving-platform to obtain large amplitudes of α and β for a given set of poses within its workspace. Therefore, maximizing $\mathscr{R}_{\mathscr{S}_2}$ is considered as the objective function for improving the task performance of the manipulator.

Design Variables

All the exit-points of the CDPR, namely, A_i and $i = 1, ..., 8$ are located on the top of $\mathscr{P}_0$ and on its rectangle vertices. The vertices, namely, $\mathscr{A}_i$ and $i = 1, 2, 3, 4$ are illustrated in Fig. 4. Moreover, we formulate all the combinations of the cable arrangement by assuming that each $\mathscr{A}_i$, $i = 1, 2, 3, 4$ accommodates two exit-points. Therefore, cables $\mathscr{C}_i$ connects A_i to B_i and $i = 1, ..., 8$. The following equation expresses the number of all the different cable arrangements.

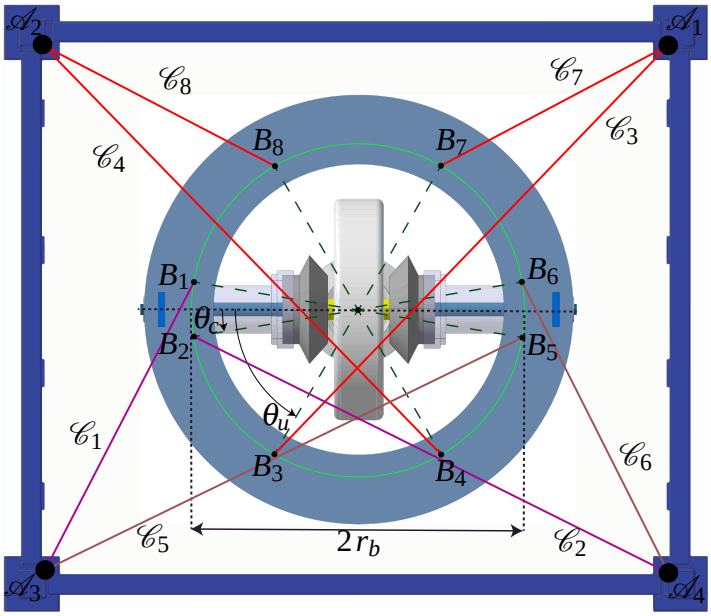

FIGURE 4: Top-view of the base frame and up-scaled moving-platform with the embedded tilt-roll wrist

$$\mathscr{N}_a = \frac{P(n,k)}{r_1!\,r_2!\,r_3!\,r_4!} = \frac{8!}{(2!)^4} = 2520 \tag{39}$$

where, the number of all the different cable arrangements is denoted as $\mathscr{N}_a$, $P(n,k)$ refers to k-permutations of n with $n = k = 8$. The number of times that $\mathscr{A}_i$, $i = 1, 2, 3, 4$ can be chosen as exit points is noted as $r_i = 2$. From Eq. (39), 2520 cable arrangements are considered for the CDPR under study. Decision variable, η is associated to the cable arrangement of the CDPR.

The geometric design variables are shown in Figs. 3 and 4. The first decision variable, namely, r_b, is the radius of the circle that passes through B_i, $i = 1, ..., 8$. h_1 denotes the height of the moving-platform. w_b is the width of the top-plate of the moving-platform. All the anchor points are located on a circle drawn on the top-plate with radius of r_b, as shown in Fig. 4. Therefore, the positions of the anchor points ${}^1\mathbf{b}_i$ are defined in polar coordinates as follows:

$${}^1\mathbf{b}_i = -r_b \begin{bmatrix} \cos\theta_i \\ \sin\theta_i \end{bmatrix} \quad i = 1, ..., 8. \tag{40}$$

The anchor point B_i is connected to exit point A_i, $i = 1, ..., 8$. The exit points of the manipulator, A_i are fixed on the top vertices of $\mathscr{P}_0$ as shown in Fig. 1.

The anchor points of the cable-loops, namely, B_1, B_2, B_5, B_6 are constrained to be close to x_1-axis in order to facilitate the actuation of $\mathscr{P}_3$ and $\mathscr{P}_4$. This constraint prevents undesired cable-loop routing. Moreover, the anchor points of the cable-loops are dependent on one another to guarantee the congruous actuation of the tilt-roll wrist as follows:

TABLE 1: Boundaries and optimum values of the design variables

Design variable	r_b	h_1	w_b	θ_c	θ_u	η
Unit	[mm]	[mm]	[mm]	[deg]	[deg]	[]
Lower-bound (lb)	5	100	3	-45	0	1
Optimum value	183	384	8	45	90	201
Upper-bound (ub)	210	400	10	45	360	2520

$$\theta_1 = -\theta_c \tag{41}$$
$$\theta_2 = \theta_c \tag{42}$$
$$\theta_5 = \pi - \theta_c \tag{43}$$
$$\theta_6 = \pi + \theta_c \tag{44}$$

with θ_c as cable loop angle.
Moreover, some constraints are defined to keep a symmetry of the anchor points B_i onto the moving-platform. The following expresses the constraints which relate the anchor points of uni-actuated cables to one another.

$$\theta_3 = \theta_u \tag{45}$$
$$\theta_4 = \pi - \theta_u \tag{46}$$
$$\theta_7 = \pi + \theta_u \tag{47}$$
$$\theta_8 = -\theta_u \tag{48}$$

with θ_u being the angle defining the location of the anchor points of the uni-actuated cables onto the moving-platform. Therefore, the location of anchor points B_i, $i = 1, \ldots, 8$, are a function of θ_c or θ_u. Finally, the decision variable vector is defined as follows:

$$\mathbf{x} = [r_b,\ h_1,\ w_b,\ \theta_c,\ \theta_u,\ \eta]^T \tag{49}$$

The minimum number of geometric variables for a given tilt-roll wrist is written in Eq. (49).

Constraints

The first non-linear constraint prevents collision of the end-effector and the top-plate, $\mathscr{P}_5$ and $\mathscr{P}_1$, respectively. Point E

placed on the tip of $\mathscr{P}_5$ is prone to undesired contact with $\mathscr{P}_1$ for some amplitudes of α and β. Hence, the following constraint is set to prevent any collision.

$$^1\mathbf{e}(\alpha,\,\beta) < 0, \quad -\pi \leq \alpha \leq \pi,\ -\pi \leq \beta \leq \pi. \tag{50}$$

Vector $^1\mathbf{e}$ denotes Cartesian coordinate of point E expressed in $\mathscr{F}_1$ as follows:

$$^1\mathbf{e} = \begin{bmatrix} -w_e \sin\beta \\ -h_e \cos\alpha - w_e \sin\alpha \cos\beta \\ -h_e \sin\alpha + w_e \cos\alpha \cos\beta - h_1 \end{bmatrix} \tag{51}$$

In order to simplify the constraint in Eq. (51), we can find α_h and β_h of the tilt-roll wrist such that point E is as close as possible to $\mathscr{P}_1$. It should be mentioned that, the z-component of $^1\mathbf{e}$ is only inspected for collision as for negative values of ^1e_z there is no contact between $\mathscr{P}_1$ and $\mathscr{P}_5$.

$$\frac{\partial}{\partial\alpha}\left(^1e_z(\alpha_h,\,\beta)\right) = 0 \quad -\pi \leq \beta \leq \pi \tag{52}$$

$$\frac{\partial}{\partial\beta}\left(^1e_z(\alpha,\,\beta_h)\right) = 0 \quad -\pi \leq \alpha \leq \pi \tag{53}$$

Therefore, the constraint in Eq. (50) can be rewritten as follows:

$$^1e_z(\alpha_h,\,\beta_h) < 0 \tag{54}$$

Actuation of the tilt-roll wrist requires tension difference at the two ends of the cable-loops. As the maximum tension difference generated in cable-loops is a function of weight of the platform and for larger m_1 the maximum tension difference and size of $\mathscr{S}_2$ is greater. Therefore, we set the second constraint to limit the overall weight of the moving-platform. The lower bound vector, $\mathbf{x}_{lb}$, and upper bound vector, $\mathbf{x}_{ub}$, of the decision variables are detailed in Table 1.

5 Results and Discussion

The optimization of problem (38) is solved by ©Matlab *ga* function. The obtained results are based on the given specification of the tilt-roll wrist and the CREATOR [1] prototype with a maximum of eight actuators.

The evolution of $\mathscr{R}_{\mathscr{S}_2}$ for different iteration of the optimization is shown in Fig. 5. The population size is equal to 200 at each generation. The optimum design variables are written in Table 1, which are associated to the geometry of the moving-platform and cable configuration. The optimum design, cable configuration of the overall manipulator and its maximal static workspaces, namely $\mathscr{S}_1$ and $\mathscr{S}_2$, are illustrated in Fig. 6. The optimum design and cable configuration of the moving platform yields 0.57 and 0.45 for $\mathscr{R}_{\mathscr{S}_1}$ and $\mathscr{R}_{\mathscr{S}_2}$, respectively.

$\mathscr{S}_2$ is the translational SW of the moving-platform for all possible orientations of the tilt-roll wrist. The ratio $\mathscr{R}_{\mathscr{S}_2}$ is illustrated as a function of m_1 and m_2 for a set of arbitrary design values of the moving-platform in Fig. 7. Figure 7 clearly shows that m_2 has a major influence on $\mathscr{S}_2$. It makes sense that the smaller m_1 and m_2, the higher $\mathscr{R}_{\mathscr{S}_2}$. However, it can be noticed that the effect of m_1 on $\mathscr{R}_{\mathscr{S}_2}$ is negligible compared to that of m_2. The maximum applied moment onto the $\mathscr{P}_3$ and $\mathscr{P}_4$ by cable-loops is proportional to the tension difference in the two segments of cable-loops. It is understood from the obtained results that, the variable gravitational wrench onto the moving-platform induced by $\mathscr{P}_5$ weight has significant impact on the size of the manipulator workspace. Moreover, the evolution of $\mathscr{R}_{\mathscr{S}_2}$ is traced as a function of r_b, θc and θ_u in Figs. 8-10.

In order to demonstrate the coupling of tensions in cable-loop and its effect on the size of SW, we study a similar setup of the manipulator with a difference in type of cables. In the proposed case, each cable-loop is substituted with two independent uni-actuated cables and consequently, the tilt-roll wrist becomes passive. The effects of cable-loops on the size of the workspace is clearly depicted in Fig. 11 with 0.86 and 0.8 for $\mathscr{R}_{\mathscr{S}_1}$ and $\mathscr{R}_{\mathscr{S}_2}$, receptively. By substituting uni-actuated cables with bi-actuated cables (cable-loops), the size of the static workspace decreases. In spite of that, the moving-platform can reach large amplitudes of the tilt and roll rotations as a result of cable-loops. It appears to be a trade-off between translation and large orientation workspaces due to the cable-loops in the fully-actuated CDPR.

TABLE 2: Given design parameters

Parameter	Abbreviation	Value
Mass of $\mathscr{P}_2$ [g]	$m_{\mathscr{P}_2}$	60
Mass of $\mathscr{P}_3$ [g]	$m_{\mathscr{P}_3}$	200
Mass of $\mathscr{P}_4$ [g]	$m_{\mathscr{P}_4}$	200
Mass of the end-effector [g]	m_2	600
Height of the end-effector [mm]	h_e	126
Width of the end-effector [mm]	w_e	20
Maximum admissible cable tension [N]	t_{max}	128
Minimum admissible cable tension [N]	t_{min}	0
Gear ratio of the wrist []	μ	1

[1] robot parallèle à Câbles ayant un gRand Espace de trAvail en Translation et en ORientation

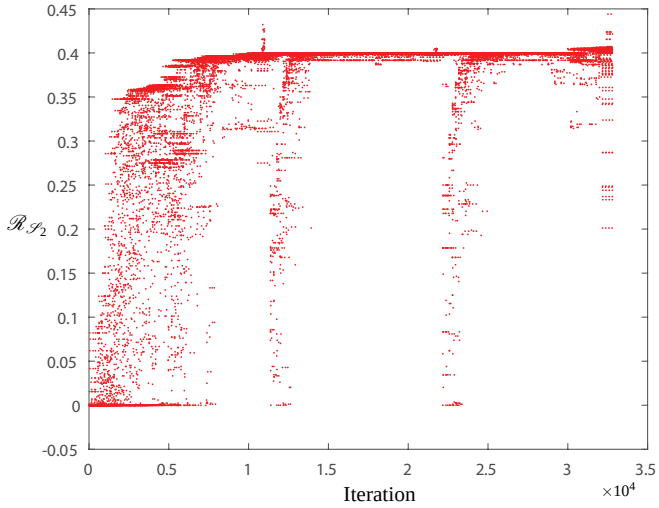

FIGURE 5: Ratio of the static workspace $\mathscr{S}_2$ as a function of the genetic algorithm iteration

It is noteworthy that translation and orientation workspaces are maximal when employing two additional actuators.

6 Prototyping

The prototyping of the moving-platform with embedded tilt-roll wrist is presented in this section. The base frame of CREATOR platform $\mathscr{P}_0$ is 4 m long (l_0), 3.5 m wide (w_0) and 4 m high (h_0) as shown in Fig. 1. Steel, aluminum alloys and ABS are used in the manufacturing of the prototype. The prototype of the moving-platform has the overall dimensions of $20 \times 20 \times 25$ cm as shown in Fig. 12. The weight of different components of the moving-platform is detailed in Table 2, and the overall weight of the moving-platform is 3.5 kg.

7 Conclusion

This paper addresses the optimum design and cable configuration of a Cable-Driven Parallel Robot (CDPR) with an embedded tilt-roll wrist for large translational and rotational workspaces. The eight-degree-of-freedom hybrid robot was studied in terms of its kinetostatic workspace. Moreover, design and prototyping of the CDPR with the embedded tilt-roll wrist was presented. The optimization results revealed that, the size of the static workspace highly relies on the specification of the tilt-roll wrist. That is to say, the variable gravitational moment of the wrist and cable-loops arrangement have crucial effects on the workspace size. It should be noted that, the considered workspace assumes no external forces on the moving-platform, except for gravity, so that the workspace analysis is relevant to

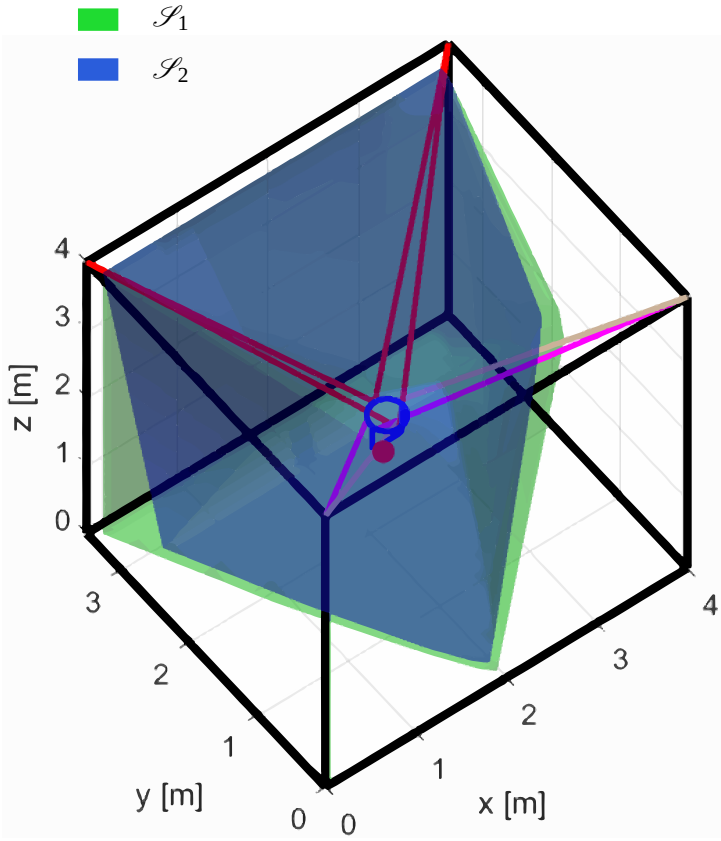

FIGURE 6: Static workspace of the optimum design of the moving-platform with cable-loop coupling effect

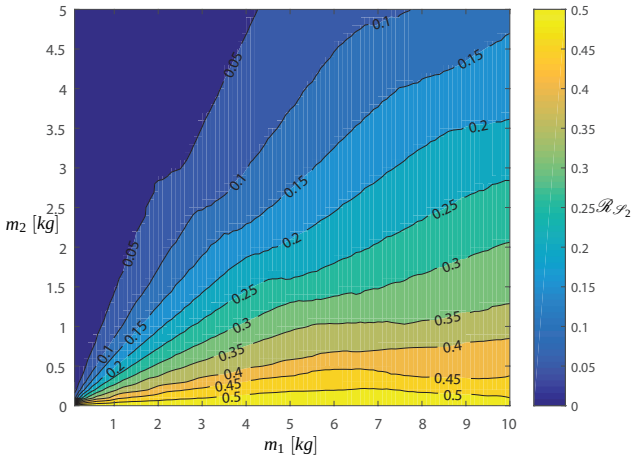

FIGURE 7: Ratio $\mathscr{R}_{\mathscr{S}_2}$ of static workspace $\mathscr{S}_2$ as a function of m_1 and m_2

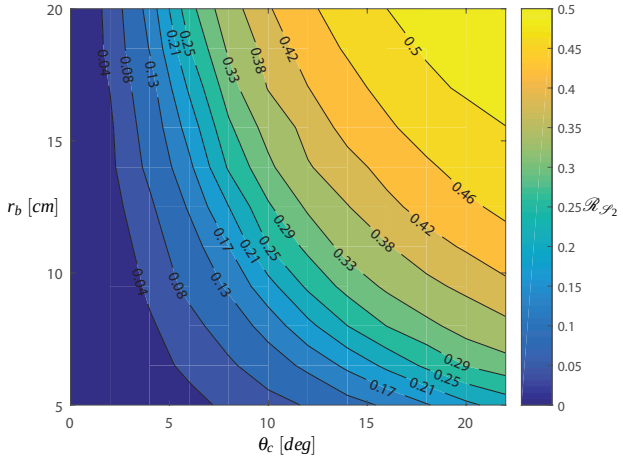

FIGURE 8: Ratio $\mathscr{R}_{\mathscr{S}_2}$ of static workspace $\mathscr{S}_2$ as a function of θ_c and r_b

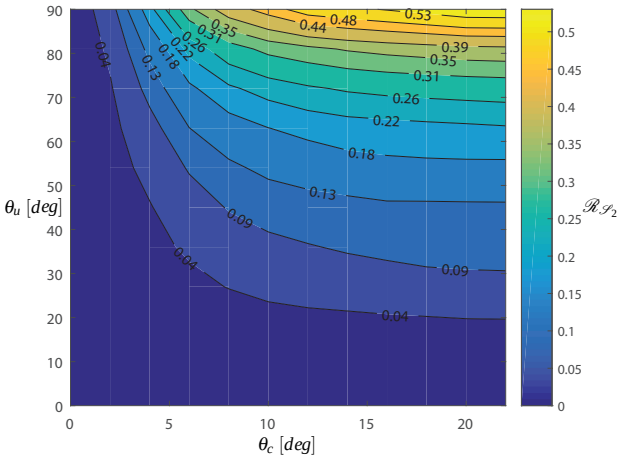

FIGURE 9: Ratio $\mathscr{R}_{\mathscr{S}_2}$ of static workspace $\mathscr{S}_2$ as a function of θ_c and θ_u

the applications such as, tomography scanning and carrying a camera.

The moving-platform is suspended by six cables and its embedded tilt-roll wrist is driven through two bi-actuated cable-loops. As a result, the end-effector covers very large rotation amplitudes about two axes without singularities. This leads to a trade-off, however, between translational and rotational workspaces due to tension coupling in cable-loops for fully-actuated CDPRs. Future work will consist in studying other factors influencing the size of the workspace, e.g., orientation of the moving-platform and over-actuation.

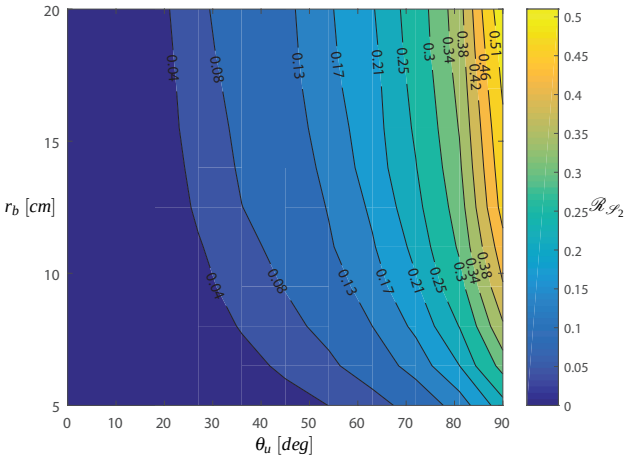

FIGURE 10: Ratio $\mathscr{R}_{\mathscr{S}_2}$ of static workspace θ_u as a function of r_b and m_2

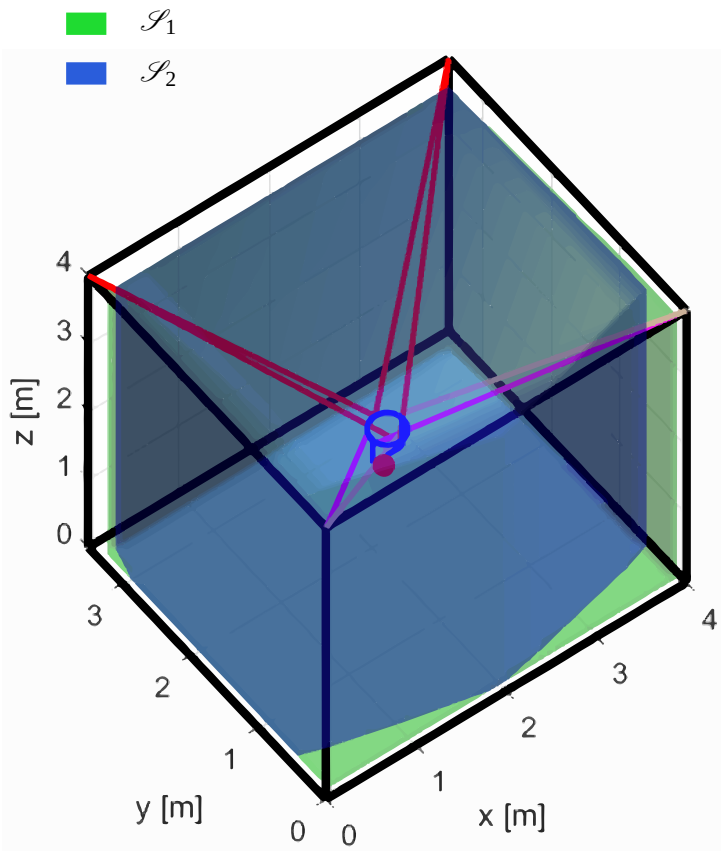

FIGURE 11: Wrench feasible workspace of the optimum design of moving-platform without cable-loop coupling effect

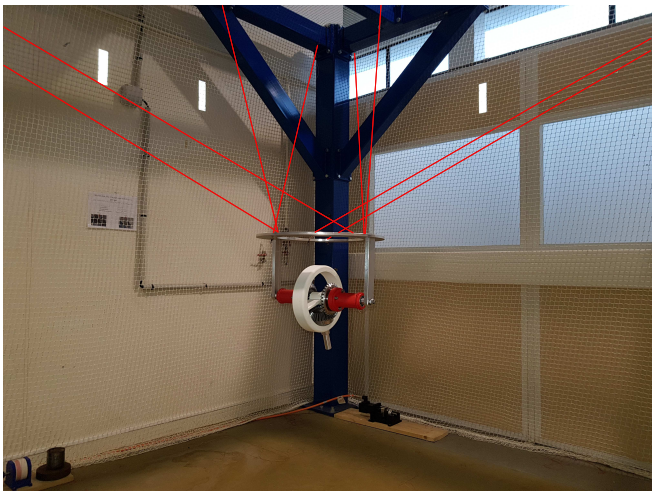

FIGURE 12: Prototype of the CDPR with an embedded tilt-roll wrist

REFERENCES

[1] Casey Lambert, Meyer Nahon, and Dean Chalmers. Implementation of an aerostat positioning system with cable control. *IEEE/ASME Transactions on Mechatronics*, 12(1):32–40, 2007.

[2] Paul Bosscher, Robert L Williams II, L Sebastian Bryson, and Daniel Castro-Lacouture. Cable-suspended robotic contour crafting system. *Automation in construction*, 17(1):45–55, 2007.

[3] Roger Bostelman, James Albus, Nicholas Dagalakis, Adam Jacoff, and John Gross. Applications of the nist robocrane. In *Proceedings of the 5th International Symposium on Robotics and Manufacturing*, pages 14–18, 1994.

[4] Lorenzo Gagliardini, Stéphane Caro, Marc Gouttefarde, and Alexis Girin. Discrete reconfiguration planning for cable-driven parallel robots. *Mechanism and Machine Theory*, 100:313–337, 2016.

[5] Sadao Kawamura, Hitoshi Kino, and Choe Won. High-speed manipulation by using parallel wire-driven robots. *Robotica*, 18(1):13–21, 2000.

[6] Angelos Platis, Tahir Rasheed, Philippe Cardou, and Stéphane Caro. Isotropic design of the spherical wrist of a cable-driven parallel robot. In *Advances in Robot Kinematics 2016*, pages 321–330. Springer, 2018.

[7] Hamed Khakpour and Lionel Birglen. Workspace augmentation of spatial 3-dof cable parallel robots using differential actuation. In *Intelligent Robots and Systems (IROS 2014), 2014 IEEE/RSJ International Conference on*, pages 3880–3885. IEEE, 2014.

[8] Hamed Khakpour, Lionel Birglen, and Souheil-Antoine Tahan. Synthesis of differentially driven planar cable parallel manipulators. *IEEE Transactions on Robotics*, 30(3):619–630, 2014.

[9] Hamed Khakpour, Lionel Birglen, and Souheil-Antoine Tahan. Analysis and optimization of a new differentially driven cable parallel robot. *Journal of Mechanisms and Robotics*, 7(3):034503, 2015.

[10] Saman Lessanibahri, Philippe Cardou, and Stéphane Caro. Kinetostatic analysis of a simple cable-driven parallel crane. In *Proceedings of the ASME 2018 International Design Engineering Technical Conferences & Computers and Information in Engineering Conference IDETC/CIE 2018*, Quebec city, Canada, August 28, 2018.

[11] Saman Lessanibahri, Philippe Cardou, and Stéphane Caro. Kinetostatic modeling of a cable-driven parallel robot using a tilt-roll wrist. In *Proceedings of CableCon 2019, 15th IFToMM World Congress*, Krakow, Poland, June 30 July 4, 2019.

[12] François Guay, Philippe Cardou, Ana Lucia Cruz-Ruiz, and Stéphane Caro. Measuring how well a structure supports varying external wrenches. In *New Advances in Mechanisms, Transmissions and Applications*, pages 385–392. Springer, 2014.

[13] Ana Lucia Cruz Ruiz, Stéphane Caro, Philippe Cardou, and François Guay. Arachnis: Analysis of robots actuated by cables with handy and neat interface software. In *Cable-Driven Parallel Robots*, pages 293–305. Springer, 2015.

[14] Shaoping Bai and Jorge Angeles. The design of a gearless pitch-roll wrist. In *Robotics and Automation, 2005. ICRA 2005. Proceedings of the 2005 IEEE International Conference on*, pages 3213–3218. IEEE, 2005.

[15] Tam Nhat Le, Hiroki Dobashi, and Kiyoshi Nagai. Configuration of redundant drive wire mechanism using double actuator modules. *ROBOMECH Journal*, 3(1):25, 2016.

[16] Peter Racioppo, Wael Saab, and Pinhas Ben-Tzvi. Design and analysis of reduced degree of freedom modular snake robot. In *ASME 2017 International Design Engineering Technical Conferences and Computers and Information in Engineering Conference*, pages V05BT08A009–V05BT08A009. American Society of Mechanical Engineers, 2017.

[17] Kiyoshi Nagai, Tam Nhat Le, Yoshikatsu Hayashi, and Koji Ito. Kinematical analysis of redundant drive wire mechanisms with velocity constraint. In *Mechatronics and Automation (ICMA), 2012 International Conference on*, pages 1496–1501. IEEE, 2012.

[18] Tam Nhat Le, Hiroki Dobashi, and Kiyoshi Nagai. Kinematical and static force analysis on redundant drive wire mechanism with velocity constraint modules to reduce the number of actuators. *ROBOMECH Journal*, 3(1):22, 2016.

[19] Saman Lessanibahri, Philippe Cardou, and Stéphane Caro. Parasitic inclinations in cable-driven parallel robots using cable loops. *Procedia CIRP*, 70:296–301, 2017.

[20] Kazuhito Hyodo and Hiroaki Kobayashi. Kinematic and

control issues on tendon controlled wrist mechanism. In *Robotics, Mechatronics and Manufacturing Systems edited by T. Takamori, K. Tsuchiya*, pages 89–94. Elsevier, 1992.